

Computer Simulations in Materials Science and Engineering

Definitions, Types, Methods, Implementation, Verification, and Validation

Lawrence E. Murr*

The University of Texas at El Paso, Metallurgical, Materials and Biomedical Engineering, El Paso, TX, USA

Abstract

Computer simulation is described as a comprehensive method for studying materials and materials systems. Computational methods used on different length and time scales for the simulation of materials structures and behavior are described along with process features involved in the implementation, verification, and validation of computer simulations. Computer simulation in the context of integrated computational materials engineering as this relates to the Materials Genome Initiative concept for materials innovation and advanced materials development and deployment is discussed.

Keywords

Computer simulations; Simulation verification and validation

Introduction

Computational physics, computational chemistry, computational materials science and chemistry, and computational materials science and engineering embody computational methods used on different length and time scales for the simulation of materials behavior. These involve the integration of materials synthesis, processing, characterization, theory, and experiments along with computer simulation and modeling. Verification and validation of various computational approaches and simulations that span the wide ranges in time and length scales are also an important aspect of computer simulations in materials sciences and engineering. A growing extension of computational materials science and engineering also involves the integration of materials information or informatics with product manufacturing process simulation and performance analysis, which in effect extends or reconfigures the materials science and engineering tetrahedral or pyramidal paradigm to one involving an octahedron as illustrated in Fig. 1. Often referred to as integrated computational materials engineering or integrated computational materials science and engineering, this multiscale modeling strategy employs computer simulations in shortening design and manufacturing cost and time as well as the implementation of new materials and manufacturing technologies.

Computational materials science and engineering, to be effective, needs to be driven by new insights and theories vested in engineering materials performance along with the other paradigm elements shown in Fig. 1. In addition, computational modeling should be routinely integrated as far as possible with experimentation and the implementation of the new materials paradigm, including characterization, which can provide real images and microstructures across the length scale in particular.

*Email: lemurr@utep.edu

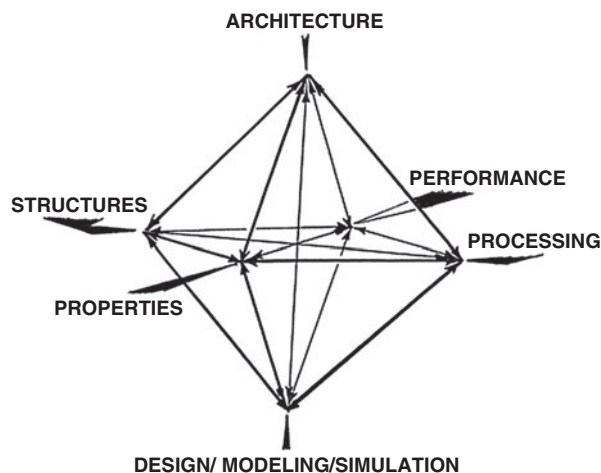


Fig. 1 The extended octahedron for materials science and engineering. See Fig. 24 in chapter “Laser and Electron Beam Melting Technologies”

In the broadest sense, computer simulation can be used for prediction, qualitative or systemic predictions, and to understand materials systems and their behavior. Predictive capability drives technological discovery and innovation in materials science and engineering. Where data is available for a materials system, computer simulation can determine how events could have occurred or how events actually did occur. Broadly speaking, computer simulation is a comprehensive method or process for studying materials systems. This process includes choosing a model and methodology for implementing the model in a form that can be executed on a computer to calculate the output of a selected algorithm or constitutive equation and finally studying and visualizing the data generated.

The starting point for a computer simulation involves the selection or development of an idealized or adequate model of the process which is embedded in a mathematical algorithm representing physical laws, state variables, or boundary conditions. When run on a computer, the selected algorithm produces a numerical picture of the system’s state as it is conceptualized in the chosen model (Humphreys and Imbert 2010). Computational modeling can provide direction in performing experiments by predicting properties of materials or a series of materials even before their processing or synthesis or indicate the futility of a synthetic route. Modeling can provide approximate answers to well-characterized materials, while experiments can provide more exact or real answers to materials which are not well characterized. In this sense, computational modeling and simulation can allow for the performance of virtual experiments.

Winsberg (2003) has concluded that “Successful simulation studies do more than compute numbers. They make use of a variety of techniques to draw inferences from these numbers. Simulations make creative use of calculational techniques that can only be motivated extra-mathematically and extra-theoretically. As such, unlike simple computations that can be carried out on a computer, the results of simulations are not automatically reliable. Much effort and expertise goes into deciding which simulations results are reliable and which are not.”

In many simulations, it is not the computing power or time in which the greatest effort is invested but rather in the selection and development of a suitable model which can be verified and validated, often by a lengthy trial-and-error method which alters the input parameters and associated algorithms within sensible ranges describing physical phenomena, especially properties of engineering materials. It is also often found that more time is involved in determining what to simulate than to actually perform the simulations. This is due in part to the fact that for many engineering materials properties, in particular, there is no adequate mathematical description to relate them in a quantitative way to microscopic phenomena. This is one of the major limitations of computer simulations in general and computational

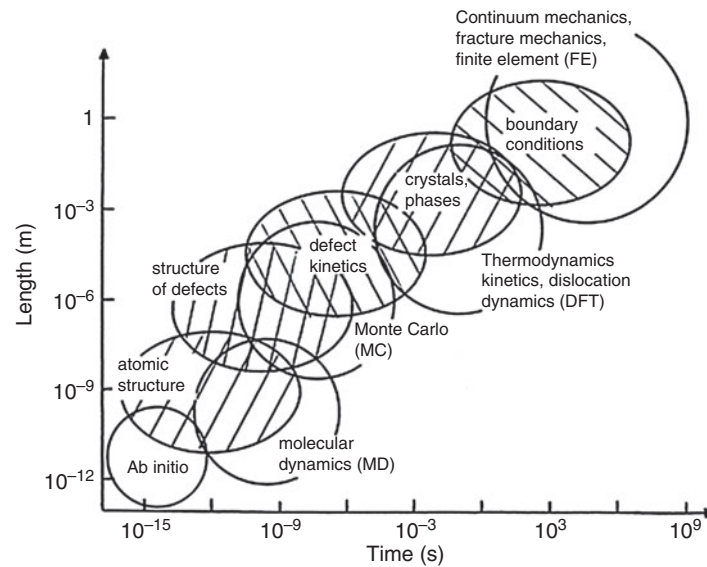


Fig. 2 Key simulation methods for length and time scales applied to materials structures and microstructures

materials science and engineering in particular. This feature is often described as a length and time scale problem but is in reality more of a lack of fundamental knowledge. Bridging the length scale from the atomic or nanoscopic to macroscopic regimes requires a fundamental understanding of the relevant phenomena characteristic of each length scale.

First-principles or *ab initio* calculations are fundamentally useful since basic data are derived from quantum mechanics (vested in the Schrödinger equation) and therefore require no experimental input on a material. Atomistic-scale computations provide primitive or fundamental information such as energies vested as heat of formation, atom positions, forces, band structures, etc., while engineering concerns are focused on higher-level properties such as ductility, strength, phase stability, resistivity, etc. Engineering properties are usually complex aggregates of the underlying atomic physics, and it is difficult in many instances to relate computational output to anything relevant in an engineering context. Simulations in materials physics are focused on understanding lattice and defect dynamics at the atomic scale, often using *molecular dynamics* (MD) or *Monte Carlo* (MC) *methods* which, as noted, often use physical potentials or force fields derived from solutions of the nonrelativistic Schrödinger equation for some limited number of atoms (Car and Parinello 1985). In contrast, and at the extreme end of the length-time scale representation shown in Fig. 2, materials-related simulations focused on engineering or large-scale materials problems resort to *finite element methods* (FEM) where the microstructure is homogenized by using averaging, constitutive relationships (Abraham et al. 1998; Bathe 1982; Bulatov et al. 1998), and related methodologies for coupling of length scales (Broughton et al. 1999). Figure 2 illustrates the major simulation methods for different length and time scales superimposed on the hierarchical features of materials microstructures and macrostructures representing materials systems of industrial interest which are highly heterogeneous and characterized by a variety of defects, interfaces, and related microstructural features (Steinhauser 2008).

In mid-2011, the USA announced *the Materials Genome Initiative*, a new effort to develop an infrastructure to accelerate advanced materials discovery and deployment. One of the major components of the Materials Genome Initiative is the development of tool sets necessary for a new research paradigm where computational analysis and simulation will decrease the reliance on conventional experimentation and testing. In addition data sharing systems and more integrated engineering teams will hopefully allow design and systems engineering as well as manufacturing strategies to be more interactive. This can be

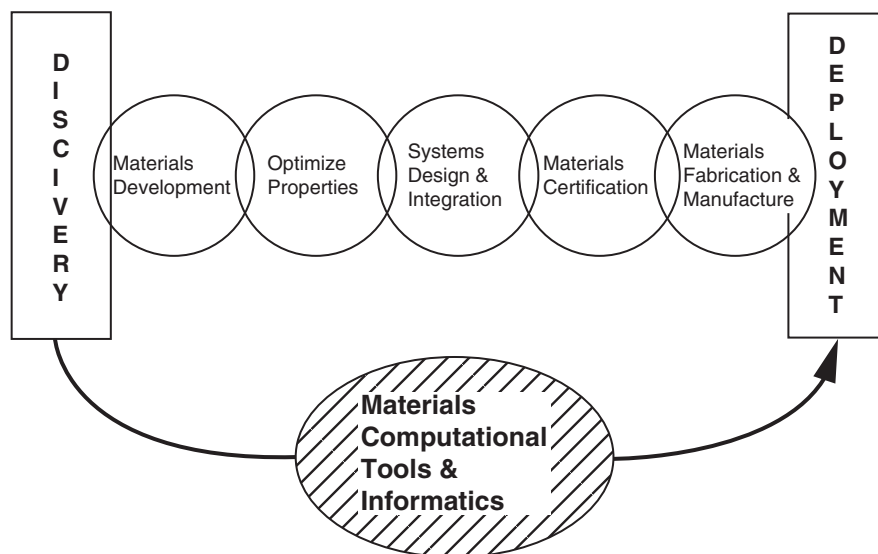


Fig. 3 Materials development model characterizing the Materials Genome Initiative

illustrated in an integrated materials design continuum model shown schematically in Fig. 3. In this model, the integration of materials computational tools and information (or informatics), especially comprehensive materials databases, will drive shorter materials development cycles from the current 10–20 years to roughly one-tenth that time frame. Materials and materials systems models simulating performance, along with appropriate model validation, especially with modular and user-friendly computational software, must be a significant part of developing a materials innovation infrastructure.

More recently, a new initiative was developed by the Minerals, Metals, and Materials Society in the USA which involves a “roadmapping study for connecting materials models and simulations across length and time scales” (Robinson 2014; TMS 2015). A similar effort to develop a materials genome concept has also been described for China (Lin 2016), while new materials modeling frontiers have been discussed by Marzari (2016), Regli et al. (2016), and Geers and Yvonnet (2016) who describe large-scale computation using computational homogenization to speed up structure-property analysis. Bonora and Brown (2014) and Calvin and Larsen (2013) also describe computational modeling of materials under extreme conditions.

Types and Methods of Computer Simulations

Two types of computer simulations are used for three general purposes: prediction, understanding, and exploration. Equation-based simulations are commonly used in the physical or materials sciences where a governing theory can guide construction of mathematical models based on differential equations. These equations are either particle based, involving discrete bodies or differential equation sets governing their interaction, or field based, where a set of equations govern the time evolution of a continuous medium or field. Correspondingly, agent-based simulations are similar to particle-based simulations, but there are no global differential equations governing the motions of individuals being studied in a social or behavioral science context (Epstein 1999). In addition, some simulation models, referred to as multiscale simulation models, couple modeling elements from different description scales. These can involve molecular dynamics (MD), quantum mechanics, or both. Many problems involving classical MD techniques are restricted to small length and time scales as implicit in Fig. 2; an edge length of a few hundred nanometers

simulated for a few nanoseconds, although one time step in a MD simulation, is typically on the order of femtoseconds ($\sim 10^{-15}$ s). An MD simulation will typically involve several million time steps and $\sim 10^{10}$ or more particles (Kadav et al. 2004).

Monte Carlo (MC) simulations are another large class of computer simulations or computer algorithms that use randomness to calculate the properties of a mathematical model and where the algorithm randomness is not a feature of the chosen model. Consequently MC simulations are not always simulations of the systems they are being used to study (Grüne-Yanoff and Weirich 2010).

Ab initio methods use quantum mechanics, and especially the Schrödinger equation, to determine the physical properties of molecules. However, the Schrödinger equation is so complex that it can only be solved analytically for a few simple cases involving simple systems and very few atoms. In the time-independent form of the Schrödinger equation

$$\nabla^2 \psi = [2m(E - V)\psi]/\hbar^2 = 0, \quad (1)$$

$$\psi = \psi(R_1, \dots, R_N, \dots, r_1, \dots, r_k, t) \quad (2)$$

where R_i and r_i denote positions of the i th nucleus and the i th electron, respectively. The variable t denotes time. Approximate solutions for the Schrödinger equation in each time step determine the effective potential energy of the nuclei. Approximate solutions are often obtained by the Hartree-Fock (HF) equation which uses the central field approximation which integrates the electron-electron repulsion, yielding an average effect instead of an explicit energy. A disadvantage of HF calculations is that the effects of one electron on another is not taken into consideration. In contrast, the so-called density functional theory (DFT) takes electron correlation into consideration in order to calculate the ground state energy of many particle systems. Other ab initio methods combine DFT with classical MD in a way that the degrees of freedom of electrons can be treated explicitly in contrast to using classical “effective potentials” between atoms which neglect the electronic movements (Kosloff 1988). DFT uses the electron density rather than the wave function to describe a molecule. With ab initio simulation methods, the only information that must be provided is the number of atoms and their positions within the system. Many codes or software packages are based on DFT, while some implement HF-based models. These include ACES II, QUANTUM ESPRESSO, VASP, and GAUSSIAN. Quantum mechanical calculations often provide a connection between the atomistic and microscopic scales (Fig. 2) by using effective interaction potentials including variations of MD and ML methods such as the discrete element method (DEM) (Cundall and Strack 1979) or dissipative particle dynamics (DPD) (Hoogerbrugge and Koelman 1992). With these methods individual particles are represented by complete clusters of atoms or molecules and are treated as classical particles which can consist of millions of atoms. Although this approach does not provide an atomistic description of molecular motion, it does represent the correct hydrodynamic behavior on long length and time scales.

Both MC and MD simulations can generate representative ensembles; MC methods are generally simpler than MD methods and do not require molecular force calculations. However, for dynamic events and the generation of nonequilibrium ensembles, MD is more appropriate. MD simulations in their simplest form involve the step-by-step numerical solution of classical Newtonian equations of motion:

$$F_i = m_i \frac{d^2 r_i}{dt^2} = -\nabla \phi(r_i - r_N), \quad (3)$$

corresponding to N particles of mass m_i having position vectors r_i , with interaction potentials, ϕ , and force

fields, $\nabla\phi$. Starting from the original Lennard-Jones potential between two particles i and j with distance $r = (r_i - r_j)$ which has the general form

$$\phi_{a,b}(r) = \alpha\epsilon \left[\left(\frac{\sigma_o}{r} \right)^a + \left(\frac{\sigma_o}{r} \right)^b \right], \quad (4)$$

where

$$\alpha = \frac{1}{a-b} \left(\frac{a^a}{b^b} \right)^{\frac{1}{a-b}}, \phi_{\min} = \epsilon \text{ and } \phi(\sigma) = 0 \quad (5)$$

the most commonly used Lennard-Jones (LJ) potential for the interaction between two particles with a distance $r = (r_i - r_j)$ is expressed by

$$\phi_{LJ}(r) = 4\epsilon \left[\left(\frac{\sigma_o}{r} \right)^{12} + \left(\frac{\sigma_o}{r} \right)^6 \right]. \quad (6)$$

Here ϵ determines the energy scale, while σ_o determines the length scale. Considering Eq. 6, the potential function for N interacting particles becomes

$$\phi(r_1 \dots r_N) = \sum_{i=1}^N \sum_{j=i+1}^N \phi_{LJ}(r) = 4\epsilon \sum_{i=1}^N \sum_{j=i+1}^N \left(\frac{\sigma_o}{r} \right)^6 \times \left(\left(\frac{\sigma_o}{r} \right)^6 - 1 \right). \quad (7)$$

The corresponding force, F_i , exerted on particle i by particle j is then given by the gradient with respect to r_i as

$$F_i = -\nabla_{r_i} \phi_{LJ}(r_1 \dots r_N) = -24 \times \epsilon \sum_{j=1}^N \sum_{j \neq i}^N \frac{1}{r^2} \left(\frac{\sigma_o}{r} \right)^6 \times \left(1 - 2 \left(\frac{\sigma_o}{r} \right)^6 \right) r_{ij}. \quad (8)$$

where $r_{ij} = (r_i - r_j)$ is the direction vector between particles i and j at positions r_i and r_j , and $r = (r_i - r_j)$. The force, F_i , on particle i is then the sum over all forces, $F_{ij} = -\nabla_{r_i} \phi$ between particle i and all other particles j :

$$F_i = \sum_{j=1, j \neq i}^N F_{ij} \quad (9)$$

Equations 6, 7, 8, and 9 represent the most crucial part of an MD simulation which has to be optimized in terms of the force calculation which determines the interacting particle pairs. Correspondingly, the analytical form of the potential which is derived from theory is then consistently adjusted to experimental findings (Maitland et al. 1981).

In the mesoscopic scale, methods based on continuum theory are used. These involve mesh-based methods such as finite element methods (FEM). Smoothed-particle hydrodynamics (SPH) represents a modern continuum method based on the conservation equations of continuum theory which avoids mesh distortion problems inherent in FEM approaches (Liu and Liu 2003).

Continuum models which describe elastic and viscoelastic behavior of solids and fluids dominate macroscale methods of simulation, particularly the discretization of the continuum into discrete elements using FEM where elements are connected together by a topological map or mesh. Here finite element interpolation functions are built upon the mesh which insures compatibility of the interpolation. Hydrocode or the so-called wave propagation codes are also utilized which decouple the stress tensor in a deviatoric and hydrostatic component. These methods are based on a solution of the continuum conservation equations of mass, momentum, and energy as well as explicit formulations of equations of state using the so-called constitutive equations or relationships. ANSYS AUTODYN software, LS-DYNA, and ABACUS software are often used in simulations involving these issues as applied to shock and impact simulation illustrated in chapter “Ballistic and Hypervelocity Impact and Penetration.” These software methods encompass a number of different numerical approaches for impact-related problems in particular, which include Lagrange, Euler, arbitrary Lagrange-Euler (ALE), Shells, and SPH numerical processors (Cook et al. 2001). These codes also contain conservation equations, constitutive equations, and failure modes which deal with fracture, spallation, and related dynamic phenomena such as dynamic recrystallization (DRX). Lagrangian codes are characterized by a referential where the computational grid deforms with the material, while in an Eulerian referential it is fixed in space. While Lagrangian codes are conceptually more straightforward, the Eulerian approach is preferential for problems involving large deformations.

It might be noted that in FEM, forces, stresses, and strains are related by writing equations in matrix form, while in finite difference (FD) methods, the derivatives or gradients are replaced by simple differences. For example, in FD a slope of a tangent derivative is replaced by a simple formula of slope of a straight line.

The plastic response in uniaxial loading can be expressed in a simple constitutive equation of the form

$$d\sigma = \left(\frac{\partial \sigma}{\partial \epsilon} \right)_{\dot{\epsilon}, T} d\epsilon + \left(\frac{\partial \sigma}{\partial \dot{\epsilon}} \right)_{\epsilon, T} d\dot{\epsilon} + \left(\frac{\partial \sigma}{\partial T} \right)_{\epsilon, \dot{\epsilon}} dT \quad (10)$$

which connects incremental changes in true axial stress, σ , to changes in true plastic axial strain, ϵ_0 ; true plastic axial strain rate, $\dot{\epsilon}$; and absolute temperature, T . The partial derivatives shown in Eq. 10 represent materials parameters and depend on the microstructure, which in turn is influenced by deformation history of the material. In this sense, the most common representation of the plastic response of a material or the stress-strain curve of a polycrystalline metal in particular is given by the Ludwik-Hollomon equations:

$$\sigma = K\epsilon^n \quad (11)$$



and

$$\sigma = \sigma_0 + K\epsilon^n, \quad (11a)$$

where σ_0 and K are constants and the exponent n is called the work-hardening coefficient. More general forms of Eq. 11a incorporating strain rate and thermal effects implicit in Eq. 10 are expressed in physically based constitutive equations such as the Johnson-Cook equation (Johnson and Cook 1983):

$$\sigma = (\sigma_0 + K\epsilon^n) \left(1 + C \ln \left(\frac{\dot{\epsilon}}{\dot{\epsilon}_0} \right) \right) \left[1 - \left(\frac{T - T_r}{T_m - T_r} \right)^m \right], \quad (12)$$

Table 1 Simulation methods and software examples associated with length scale applications

Scale (m)	Simulation methods/software	Application examples
Electronic/atomistic		
~10 ⁻¹² – 10 ⁻⁹	Self-consistent Hartree-Fock (SC-HF) and self-consistent DFT/CRYSTAL, GAUSSIAN, Q-CHEM, VASP (Phillips 2003; Steinhauser 2008), ab initio MD/MOLPRO Quantum MC (Nightingale and Umrigar 1999)	Crystal ground state, molecular structures and geometry, electronic properties, chemical reactions, energy of formation, structural energetics
Atomistic/microscopic		
~10 ⁻⁹ – 10 ⁻⁶	MD; MC using classical force fields; hybrid MD/MC Embedded atom method (EAM) (Daw 1988; Steinhauser 2008)	Equations of state, rheology, transport properties, phase equilibrium, and phase stability
Microscopic/mesoscopic		
~10 ⁻⁸ – 10 ⁻¹	MD and MC using effective force fields (Steinhauser 2008). Dissipative particle dynamics (Hoogerbrugge and Koelman 1992). Finite element methods (FEM) including microstructural features (Phillips 2003)/ABACUS. SPH, dislocation dynamics, discrete element method (DEM) (Cundall and Strack 1979)	Granular matter, fracture mechanics, grain growth and grain boundaries, polycrystal elasticity and plasticity, phase transformations, diffusion, dislocations, motion of interfaces
		
~10 ⁻⁶ – 10 ⁰		
Mesoscopic/macrosopic		
~10 ⁻³ – 10 ²	Hydrodynamics, computational fluid dynamics; FEM/ANSYS AUTODYN, DYNA FDM/WONON, HEMP; Percolation and cluster models (Benson 1992)	Macroscopic flow, elasticity and plasticity, fracture mechanics, fatigue and wear, impact and penetration, shock wave phenomena
		
~10 ⁻⁶ – 10 ⁰		

See TMS (2015) for updated software descriptions and properties

Adapted from Steinhauser and Hiermaier (2009). See text for method abbreviations

where K , C , n , and m are material parameters, T_r is a reference temperature, T_m is the melting point, and $\dot{\epsilon}_0$ is the reference strain rate. The three groups of terms in Eq. 12 represent the work-hardening (Eq. 11a), strain rate, and thermal effects, respectively. There are other constitutive equations which incorporate microstructural issues such as grain size and dislocation effects. Zerilli and Armstrong (1992) developed two microstructurally based constitutive equations based on the framework of thermally activated dislocation motion in the context of temperature and strain-rate response of FCC and BCC metals:

$$\left. \begin{aligned} \text{FCC} : \sigma &= \sigma_G + C_2 \epsilon^{0.5} \exp(-C_3 T + C_4 T \ln \dot{\epsilon}) + K D^{0.5} \\ \text{BCC} : \sigma &= \sigma_G + C_1 \exp(-C_3 T + C_4 T \ln \dot{\epsilon}) + C_5 \epsilon^n + K D^{0.5} \end{aligned} \right\} \quad (13)$$

where σ_G and C_i ($i = 1-5$) are material constants, T is the temperature, and D is the grain size. The difference between the FCC and BCC equations (Eq. 13) is that the plastic strain is uncoupled from the strain rate and temperature for BCC metals.

Table 1 provides a brief overview of some of the more prominent and different simulation techniques and software packages used on various length scales in materials and chemical sciences, along with representative applications. This overview represents a spatial rather than a physical classification. These software systems and hydrocodes can be 1D, 2D, 3D, or in combination. Many are 2D and 3D, including the many FE and FD methods.

One of the more significant modeling methods has involved density functional theory (DFT) applications in predicting properties of crystalline materials such as energies of formation, lattice parameters, band structures, etc. The so-called high-throughput (HT) DFT calculations have generated large databases of DFT-predicted materials properties, including the Open Quantum Materials Database (OQMD) (available at <http://oqmd.org>), which currently contains predicted crystallographic parameters and formation energies for over 200,000 structures, and the Inorganic Crystal Structure Database (ICSD) (Saal et al. 2013).

It is also important to briefly discuss computational methods applied to materials thermodynamics and especially thermodynamic phase stability applications of first-principles calculations, including DFT. These relate to the advent of the calculation of phase diagrams (CALPHAD) method (Wang et al. 2013), especially modern versions of PANDAT software (Cao et al. 2009) for multicomponent phase diagram calculation and materials property simulation. Cao et al. (2009) have recently described the CALPHAD approach to require the information of the Gibbs free energies of all phases as functions of temperature and chemical composition, where the general form of the Gibbs free energy for a phase α in the CALPHAD approach is expressed as

$$G^\alpha = {}^0G^\alpha + \Delta G^\alpha, \quad (14)$$

where G^α is the Gibbs free energy of the multicomponent α phase, ${}^0G^\alpha$ represents the mechanical mixing of individual species, and ΔG^α represents interactions among the species or end-members. Following this approach

$${}^0G^\alpha = \sum x_i {}^0G_i^\alpha \quad (15)$$

and

$$\Delta G^\alpha = \Delta G_{\text{conf}}^\alpha + \sum_i \sum_{j>i} x_i x_j \sum_{n=0}^n L_{ij}^\alpha (x_i - x_j)^n + \sum_i \sum_{j>i} \sum_{k>j} x_i x_j x_k L_{ijk}^\alpha; \quad (16)$$

where x_i is the mole fraction of species i , ${}^0G_i^\alpha$ is the Gibbs free energy of species i in the structure of phase α , $\Delta G_{\text{conf}}^\alpha$ is the configurational contribution, and ${}^nL_{ij}^\alpha$ and ${}^nL_{ijk}^\alpha$ are binary and ternary interaction parameters which can be temperature dependent. $\Delta G_{\text{conf}}^\alpha$ is usually assumed to be from the ideal atomic configurational entropy of mixing given by

$$-T\Delta S_{\text{conf}} = RT \sum x_i \ln x_i, \quad (17)$$

where R is the gas constant, T is temperature, and ΔS_{conf} represents the ideal atomic configurational entropy. In modeling multicomponent atomic mobility, molar volume, and elastic coefficients using CALPHAD, the configurational contribution represented in Eq. 17 can be neglected (Wang et al. 2013).

Computational methods such as MD and DFT have also been applied to investigations of theoretical and practical aspects of solidification phenomena and simulation of solidification across the length scales where FEM is also used to investigate the die-filling and solidification processes involved with a wide range of components spanning from automotive to aeroengine turbine blades (Dantzig and Rappaz 2009). At the atomic level, MD and DFT can investigate the solid/liquid interface and its effect on microstructural morphology, while FEM and related simulations attempt to bridge the gap between solidification pattern formation at the scale of dendrite and process models involved with thermal transport and mass transport at the mesoscale and above.

It should also be pointed out that practical simulations, or engineering simulations, involve a wide range of computer-aided design (CAD) software such as Materialise and SolidWorks described and illustrated in chapter “Rapid Prototyping Technologies: Solid Freedom Fabrication” in connection with additive manufacturing involving the array of 3D printing technologies. SolidWorks Simulation is an FEM to calculate component displacements, stresses, and strains under internal and external loads. This software is tightly integrated with SolidWorks 3D CAD so that geometry to be analyzed is discretized using tetrahedral (3D), triangular (2D), and beam elements and solved by either a direct sparse or iterative solver involving linear or nonlinear stress analysis.

While this section has presented an overview of computer simulation methods, there has been no attempt to provide any tutorial-like descriptions of either these methods or their arrays of applications in materials science and engineering. For more detailed descriptions and applications, the reader is referred to the recent introductory overview by LeSar (2014) as well as the description and application examples provided in Phillips (2003) and Steinhauser (2008). The following section of this chapter will illustrate a few examples of implementing simulation methods as well as issues related to verification and validation of simulations and simulation methods.

Implementation, Verification, and Validation of Simulations

It is often said that *simulations without validation are nothing more than animation*. While validation on the one hand involves the process of determining whether the selected model represents the real situation, verification, on the other hand, involves the process of determining whether the simulation approximates true solutions to the differential equations representing the original model. Validation involves comparing a model output with experimental or observable data. Roy (2005) has posed that “verification deals with mathematics and addresses the correctness of the numerical solution to a given model. Validation, on the other hand, deals with physics and addresses the appropriateness of the model in reproducing experimental data. Verification can be thought of as solving the chosen equations correctly, while validation is choosing the correct equations in the first place.” In practice, the successful implementation of a model or simulation method is determined by trial-and-error adjustment between the model and the method of calculation. Consequently, it is often difficult to separate verification and validation in achieving a successful simulation. Indeed, a simulation which accurately depicts complex phenomena invariably contains a wealth of information related to that phenomena. Winsberg (2010) has recently argued that when there is relevant background knowledge in place, a simulation can actually provide more reliable knowledge of a system than an experiment. In effect, simulations can run a large number of experiments involving many variables, but there must be some basis for validation; otherwise, the experiments represented by the simulations will be largely fictitious and unrepresentative of the real world or real materials, where materials are the focus.

In chapter “Ballistic and Hypervelocity Impact and Penetration,” Fig. 14, a 3D computer simulation sequence was presented for a 3.18 mm diameter stainless steel (SS) projectile impacting a thick (semi-infinite) Ni target at a velocity of 3.4 km/s. It might be instructive to illustrate how this simulation or simulation sequence was implemented using a 3D AUTODYN (version 5.0) software package and subsequently validated (and verified). The starting point involved the actual impact experiments utilizing 3.18 mm diameter (spherical) 440 stainless steel projectiles launched at different velocities from either a powder propellant gun or gas gun at normal incidence against 2.5 cm thick stationary Ni targets. These impacted targets were cut in half and observed in the scanning electron microscope (SEM) to examine the fragmentation of the projectile and deposition within the excavated crater, at different impact velocities (Hernandez et al. 2006).

The AUTODYN computer simulation involved first selecting processors corresponding to the projectiles and the Ni target. The smoothed-particle hydrodynamic (SPH) processor with a simple principal stress failure model used to model the projectile was coupled with a Lagrangian target model where the grid distorts with the target material. An erosion algorithm was also implemented to alleviate grid tangling and element degeneracy. This algorithm works by removing Lagrangian cells that have reached a user-prescribed strain (Hayhurst et al. 1995). SPH was used to model the projectile because it was assumed that it would undergo very large deformation without the need for additional algorithms such as an erosion algorithm.

A polynomial equation of state was chosen for the Ni target, while the shock equation of state was used for the 440 SS projectile:

$$U_s = C_o + S U_p, \quad (18)$$

where U_s is the shock velocity, C_o is the sound velocity, S is an empirical parameter related to the Grüneisen parameter, and U_p is the particle velocity. The Johnson-Cook strength model (or constitutive equation (Eq. 12)) was applied to the SS projectile in the form:

$$\sigma = \left[A + B \varepsilon_p^n \right] \left[1 + C \ln \dot{\varepsilon}_p^* \right] \left[1 - T_H^m \right], \quad (19)$$

where ε_p is the effective plastic strain, $\dot{\varepsilon}_p^*$ is the normalized effective plastic strain rate (Eq. 12), and T_H is the homologous temperature defined as

$$T_H = (T - T_{\text{room}}) / (T_{\text{melt}} - T_{\text{room}}), \quad (20)$$

and A , B , C , n , and m are material constants given in the AUTODYN software material library.

The Ni targets were modeled using the Steinberg-Guinan strength model where the constitutive relationships for the shear modulus, G , and the yield stress, σ , at high strain rates, are given by (Steinberg et al. 1980)

$$G = G_o \left[1 + \left(G'_p / G_o \right) P / \eta^{1/3} + \left(G'_T / G_o \right) (T - 300) \right] \quad (21)$$

and

$$\sigma = \sigma_o \left[1 + \left(\sigma'_p / \sigma_o \right) P / \eta^{1/3} + \left(G'_t / G_o \right) (T - 300) (1 + \beta \varepsilon)^n \right], \quad (22)$$

subject to $\sigma_o(1 + \beta \varepsilon)^n \leq \sigma_{\text{max}}$, where ε is the effective plastic strain, T is the temperature (K), η is the compressibility equal to V_o/V , and the primed parameters with subscripts p and T are derivatives of that parameter with respect to pressure (P) and temperature (T) at the reference state ($T = 300$ K, $P = 0$, $\varepsilon = 0$). The subscript zero also refers to values of G and σ at the reference state. Values for these parameters are also given in the AUTODYN software materials library as input parameters. These are listed for the 440 SS projectile and Ni targets shown in Table 2.

Figure 4a illustrates the 440 SS projectile and Ni target 3D-half-section model for the computer-simulated impact and their corresponding processors. Figure 4b shows a 3D-half-section SEM view for a 440 SS projectile impacting a Ni target at 3.4 km/s observed in the SEM showing the SS fragments in the crater wall. Correspondingly, Fig. 4c–f shows SEM 3D-half-section views for SS projectiles impacting Ni targets at velocities indicated above, where Fig. 4f corresponds to Fig. 4b. In Fig. 4g–j, the computer-

Table 2 Material input parameters for 3D impact crater simulation

Parameter	Stainless steel	Nickel target
	Projectile	
Equation of state	Shock	Polynomial
Strength model	Johnson-Cook	Steinberg-Guinan
Steinberg-Guinan		
Reference density (g/cm ³)	7.86	8.9
Reference temperature (K)	300	300
Specific heat (Terg/gK)	4.77E-06	4.01E-06
Shear modulus (Mbar)	8.18E-01	6.50E-01
Yield stress (Mbar)	1.00E-01	1.70E-03
Maximum yield stress (Mbar)	3.00E-02	
Hardening constant (Mbar)	20	4.60E + 01
Hardening exponent	2.50E-01	5.30E-01
Strain rate constant	1.20E-02	
Thermal softening exponent	7.50E-01	
Melting temperature (K)	2,370	2,330
Failure model	Principal stress	None
Erosion (instantaneous)	None	Inst. geometrical
Erosion strain		1.5

After Hernandez et al. (2006)

Table 3 Experimental and simulated impact crater data based on Fig. 4c–j for 440 SS projectiles impacting Ni targets

Impact velocity, U _o (km/s)	Experimental (p/D _c)	Simulated (p/D _c)
0.52	0.52	0.52
1.10	0.59	0.60
2.20	0.61	0.62
3.4	0.57	0.61

After Hernandez et al. (2006)

simulated 3D-half-section views corresponding to Fig. 4c–f are reproduced. Simply comparing the real SEM 3D-half-section views in Fig. 4c–f and the computer-simulated views in Fig. 4g–j provides a high level of verification and simulation validation. By considering the crater geometry or crater depth/crater diameter ratio (P/D_c), simple numerical comparisons can also be made as shown in Table 3 where the largest variance of 7% is observed for the 3.4 km/s impact corresponding to Fig. 4f–j or 93% validation based on this simple ratio.

Although Fig. 4 illustrates a relatively simple example of computer simulation validation related to materials, it provides a broader perspective for simulations which can relate to time or events within some time frame, as shown in Fig. 14 of chapter “Ballistic and Hypervelocity Impact and Penetration” which illustrates the formation of the crater in Fig. 4f–j. This feature of computer simulation is particularly unique and especially useful in the context of dynamic events such as impact since in reality there are only two end points: the projectile striking the target surface at time, t equal zero, and the fully formed crater at some steady-state time. Consequently, validation of a computer simulation for a particular materials system can allow for the detailed event sequence to be examined in some time interval or time sequence. These features are illustrated for related impact events in Figs. 14, 24, 26d, and 28 of chapter “Ballistic and

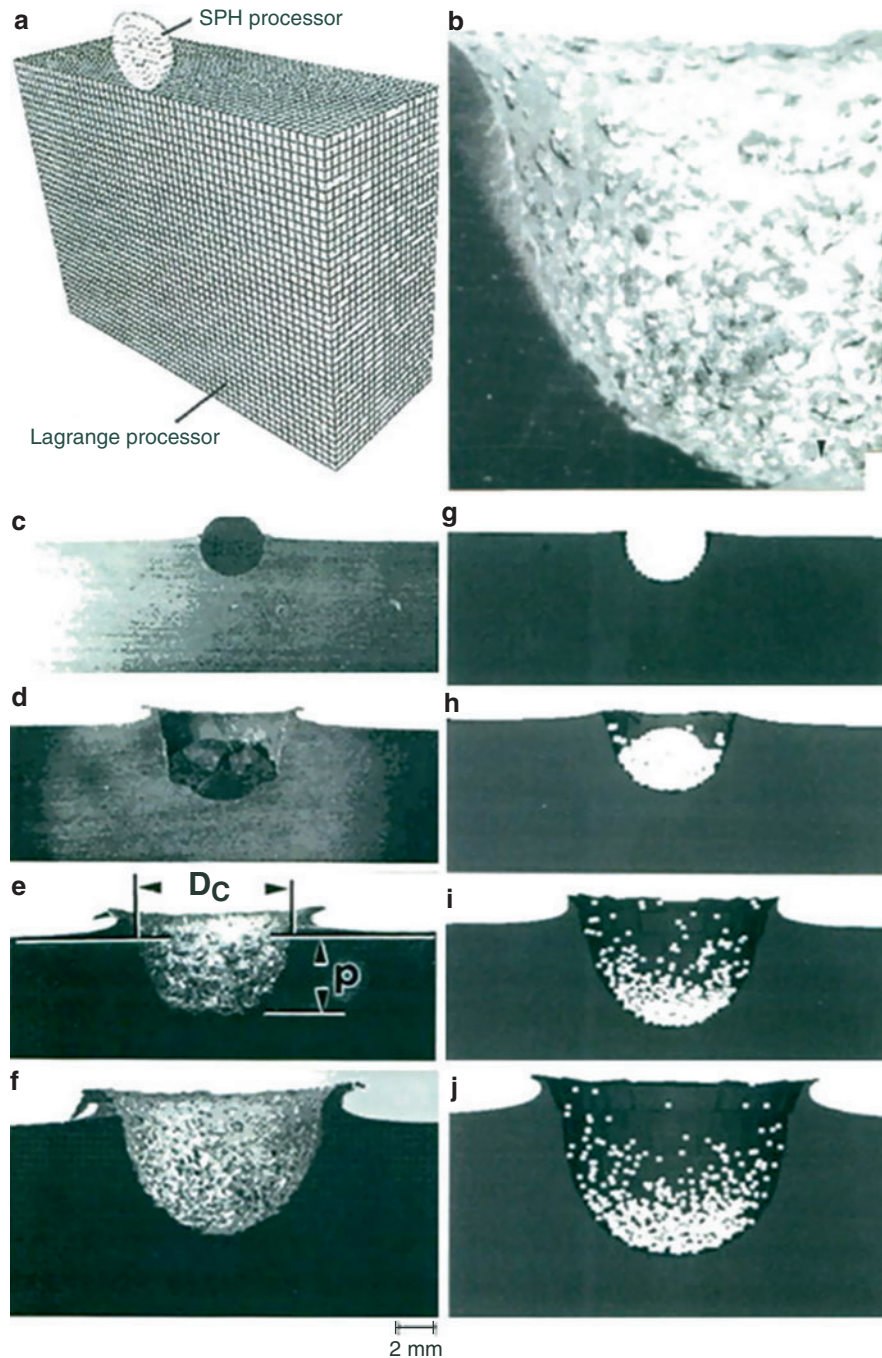


Fig. 4 (a) Projectile/target 3D-half-section model for computer-simulated impact. (b) SEM view of 3D-half-section of Ni crater with 440 SS projectile fragments after impact at 3.4 km/s. (c–f) Show experimental, SEM 3D-half-section views at impact velocities of 0.52, 1.1, 2.2, and 3.4 km/s, respectively. (g–j) Show computer-simulated 3D-half-section views at impact velocities of 0.52, 1.1, 2.2, and 3.4 km/s, respectively (Adapted from Hernandez et al. (2006))

Hypervelocity Impact and Penetration.” Figures 22, 26, 28a–c, and 29 of chapter “Ballistic and Hypervelocity Impact and Penetration” have also shown examples of 2D computer simulation validation for related impact events in materials systems. It must be cautioned that valid simulations for one materials

system are not necessarily applicable or able to be extrapolated to another different materials system, although, as illustrated in Fig. 4, it may be possible to validate only one or a few experimental events to allow the simulation to be applied in other circumstances involving initial impact or related physical conditions.

References

- Abraham F, Broughton J, Bernstein N, Kaxiras E (1998) Spanning the length scales in dynamic simulation. *Comput Phys* 12:538–556
- Bathe K (1982) *Finite element procedures in engineering analysis*. Prentice Hall, Cambridge, UK
- Benson DJ (1992) *Computational methods in Lagrangian and Eulerian hydrocodes*. *Comput Methods Appl Mech Eng* 99(2–3):235–394
- Bonora N, Brown E (eds) (2014) *Numerical modeling of materials under extreme conditions*. Springer, New York
- Broughton JQ, Abrahams FF, Bernstein N, Kaxiras E (1999) Concurrent coupling of length scales; methodology and applications. *Phys Rev B* 60:2391–2403
- Bulatov VU, Abraham F, Kubin L, Devrince B, Yip S (1998) Connecting atomistic and mesoscale simulations of crystal plasticity. *Nature* 391:669–672
- Calvin J, Larsen J (2013) *Extreme physics: properties and behavior of matter at extreme conditions*. Cambridge Univ Press, Cambridge, UK
- Cao W, Chen S-L, Zhang F, Wu K, Yang Y, Chang YA, Schmid-Fetzer R, Oates WA (2009) PANDAT software with PanEngine, PanOptimizer and PanPrecipitation for multi-component phase diagram calculation and materials property simulation. *CALPHAD Comput Coupling Phase Diagr Thermochem* 33:328–342
- Car R, Parinello M (1985) Unified approach for molecular dynamics and density-functional theory. *Phys Rev Lett* 55:2471–2474
- Cook RD, Malkus DS, Plesha ME, Witt RJ (2001) *Concepts and applications of finite element analysis*, 4th edn. Lavoisier SAS, Paris
- Cundall P, Strack O (1979) A discrete numerical model for granular assemblies. *Geotechnique* 29:47–65
- Dantzig JA, Rappaz M (2009) *Solidification*. CRC Press/Taylor and Francis Group, LCC, Boca Raton
- Daw MS (1988) Model of metallic cohesion: the embedded atom method. *Phys Rev B* 39:7441–7452
- Epstein J (1999) Agent-based computational models and generative social science. *Complexity* 4(5):41–57
- Geers MGD, Yvonnet J (2016) Multiscale modeling of microstructure-property relations. *MRS Bull* 41(8):610–616
- Grüne-Yanoff T, Weirich P (2010) Philosophy of simulation. *Simul Gaming Interdiscip J* 41(1):1–31
- Hayhurst CJ, Ranson HJ, Gardner DJ, Birnbaum NK (1995) Modeling of microparticle hypervelocity oblique impacts on thick targets. *Int J Impact Eng* 17:375–386
- Hernandez VS, Murr LE, Anchondo IA (2006) Experimental observations and computer simulations for metallic projectile fragmentation and impact crater development in thick metal targets. *Int J Impact Eng* 32:1981–1999
- Hoogerbrugge P, Koelman J (1992) Simulating microscopic hydrodynamic phenomena with dissipative particle dynamics. *Europhys Lett* 19:155–160
- Humphreys P, Imbert C (eds) (2010) *Models, simulations and representations*. Routledge Publishers, London

- Johnson GR, Cook WH (1983) A constitutive model and data for metals subjected to large strains, high strain rates and temperatures. In: Proceedings of the 7th international symposium. O Ballistics, The Hague
- Kadau K, Germann T, Lomdahl P (2004) Large-scale molecular dynamics simulation of 19 billion particles. *J Mod Phys C* 15:193–201
- Kosloff R (1988) Time-dependent quantum-mechanical methods for molecular dynamics. *J Chem Phys* 92:2087–2100
- Le Sar R (2014) Introduction to computational materials science. Cambridge University Press, Cambridge, UK
- Lin H-Q (2016) Boosting computational capabilities. *Nat Mater* 15:693–694
- Liu GR, Liu MB (2003) Smoothed particle hydrodynamics. A meshfree particle method. Scientific, Singapore
- Maitland G, Rigby M, Smith E, Wakeham W (1981) Intermolecular forces – their origins and determination. Clarendon Press, Oxford
- Marzari N (2016) Materials modelling: the frontiers and the challenges. *Nat Mater* 15:381–382
- Nightingale M, Umrigar C (eds) (1999) Quantum Monte Carlo methods in physics and chemistry. Springer, New York
- Phillips R (2003) Crystals, defects and microstructures – modeling across scales. Cambridge University Press, Cambridge, UK
- Regli W, Rossignac J, Shapiro V, Srinivasan V (2016) The new frontiers in computational modeling of materials structures. NISTIR 8110, Natl Inst of Standards and Technol, U. S. Dept of Commerce, Washington, DC. Feb, 2016, 24pp
- Robinson L (2014) New TMS study tackles the challenge of integrating materials simulations across length scales. *JOM* 66:1356–1359
- Roy S (2005) Recent advances in numerical methods for fluid dynamics and heat transfer. *J Fluids Eng* 127(4):629–630
- Saal JA, Kirklin S, Aykol M, Meredig B, Wolverton C (2013) Materials design and discovery with high-throughput density functional theory: the open quantum materials database (OQMD). *JOM* 65(1):1501–1509
- Steinberg DJ, Cochran SG, Guinan MW (1980) A constitutive model for metals applicable at high strain rates. *J Appl Phys* 51(3):1498–1502
- Steinhauser MO (2008) Computational multiscale modeling of solids and fluids – theory and applications. Springer, Heidelberg
- Steinhauser MO, Hiermaier S (2009) A review of computational methods in materials sciences: examples from shock-wave and polymer physics. *Int J Mol Sci* 10:5135–5216
- TMS (2015) Modeling across scales: a roadmapping study for connecting materials models and simulations across length and time scales. The Minerals, Metals and Materials Society (TMS), Warrendale
- Wang Y, Shang S, Chen L-Q, Liu Z-K (2013) Density functional theory-based database development and CALPHAD automation. *JOM* 65(1):1533–1539
- Winsberg E (2003) Simulated experiments: methodology for a virtual world. *Philos Sci* 70:105–125
- Winsberg E (2010) Science in the age of computer simulation. The University of Chicago Press, Chicago
- Zerilli FJ, Armstrong RW (1992) The effect of dislocation drag on the stress-strain behavior of fcc metals. *Acta Met Mater* 40:1803–1809